applied sciences

MDPI

Article

Seasonal and Intra-Annual Patterns of Sedimentary Evolution in Tidal Flats Impacted by Laver Cultivation along the Central Jiangsu Coast, China

Wanyun Lu [1,2,3], Jiaqi Sun [1,2], Yongxue Liu [1,3,4,*], Yongchao Liu [1,2,3] and Bingxue Zhao [1,2,3]

1 School of Geography and Ocean Science, Nanjing University, Nanjing 210023, Jiangsu Province, China; wanyunlu@smail.nju.edu.cn (W.L.); mg1527062@smail.nju.edu.cn (J.S.); yongchaoliu@smail.nju.edu.cn (Y.L.); dg1827049@smail.nju.edu.cn (B.Z.)
2 Key Laboratory of Coastal Zone Exploitation and Protection, Ministry of Natural Resources of China, Nanjing 210024, Jiangsu Province, China
3 Collaborative Innovation Center of South China Sea Studies, Nanjing University, Nanjing 210023, Jiangsu Province, China
4 Jiangsu Center for Collaborative Innovation in Geographical Information Resource Development and Application, Jiangsu Province, Nanjing 210023, China
* Correspondence: yongxue@nju.edu.cn; Tel.: +86-25-89881181

Received: 22 October 2018; Accepted: 26 January 2019; Published: 3 February 2019

check for updates

Abstract: Human activities such as the rapid development of marine aquaculture in the central Jiangsu coast have had a marked impact on the tidal flat morphology. This research focuses on characterizing the spatial expansion of laver cultivation and its influence on the sedimentary evolution of tidal flats in the central Jiangsu coast. First, seasonal digital elevation models (DEMs) were established using 160 satellite images with medium resolution. Then, laver aquaculture regions were extracted from 50 time-series satellite images to calculate the area and analyze the spatial distribution and expansion of these areas. Finally, seasonal and intra-annual sedimentary evolution patterns of both aquaculture and non-aquaculture regions were determined using the constructed DEMs. Our results show that aquaculture regions have gradually expanded to the north and peripheral domains of the entire sand ridge since 1999 and by 2013, the seaward margins of each sandbank developed into dense cultivation regions. Additionally, the aquaculture regions increased from 11.99 km^2 to 295.28 km^2. The seasonal sedimentary evolution patterns indicate that deposition occurs during the winter and erosion during the summer. Thus, the aquaculture regions experience deposition in certain elevation intervals during the laver growing period and in the non-growing period, alluvial elevation intervals in the aquaculture regions are eroded and erosive ones are deposited in order to maintain the balance between scouring and silting. The sedimentary evolution of each sandbank is heterogeneous due to their different locations and the difference in sediment transport. The intra-annual evolution pattern is characterized by deposition in the high tidal flats and erosion in low ones. Hydrodynamic conditions and laver cultivation dominate partial sedimentary evolution, which gradually shapes the beach surface.

Keywords: tidal flats; human activities; laver cultivation; spatial expansion; seasonal and intra-annual evolution patterns

1. Introduction

Tidal flats are broad areas between the mean high tide and mean low tide levels [1], which are the most promising areas for ocean exploitation [2]. They provide developmental space for fisheries, agricultural land and harbor construction, as well as serve ecological and environmental functions [3,4].

In addition, tidal flats play an important role in protecting the coast [5]. However, due to natural factors and increasingly intensive human activities, tidal flats are dynamically affected and facing grim challenges [6,7]. Numerous deltas around the world are undergoing erosion [8–12] due to decreasing sediment supply. Moreover, natural factors (e.g., typhoon-induced storm surges in summer and winter storms) have impacts on stabilization of tidal flats seasonally by increasingly scouring the surface of tidal flats [13,14]. On the other hand, human activities have greatly changed the equilibrium state of the coastal sedimentary environment, which exerts a significant impact on the ecosystem and the geomorphic evolution of tidal flats. Understanding the changes in the topography of the mudflat can provide fundamental information and scientific evidence for environmental management, tidal-flat protection, coastal development and economic exploitation [15].

The central Jiangsu coast is a typical tidal area in China, whose abundant coastal wetlands provide natural resources suitable for large-scale aquaculture, especially seafood farming. Due to these characteristics, this region has now been established as a unique industrial belt specializing in coastal aquaculture. Laver cultivation is a representative of aquaculture industries in Jiangsu and expands rapidly. The species' name is porphyra yezoensis, which is the primary algae cultivated in north of the Yangtze River. To grow laver, pillars and semi-floating rafts are constructed in the intertidal zone, while full-floating rafts are used in the subtidal zone. Plentiful net screens and bamboo poles are required no matter which kind of cultivation method is employed. Before cultivation, bamboo poles were inserted into the silt and net screens were laid on the poles to provide space for laver growing. Given the scale of these constructions with frequent inserting and pulling out bamboo poles and with the expansion of aquaculture in the region, it is worthwhile to study whether large-scale laver cultivation will affect the sediment environment in the central Jiangsu coast.

Presently, studies relating to the impact of human activities on the sediment, hydrodynamics and ecological environment of tidal flats have concentrated on (1) artificial reclamation [16–22], (2) artificial introduction of plants [23–26], (3) seawall construction and repair [27–29] and (4) harbor and wind farm construction [30,31]. Despite significant interest, the effect of artificial seafood cultivation on the geomorphic evolution process has not been sufficiently studied and lacks thorough analysis due to the difficulty of data acquisition. To explore the effect of laver aquaculture on the sedimentary evolution of tidal flats, it is necessary to analyze the surface of tidal flats. At present, the surface evolution detection method of tidal flats mainly uses SAR and LIDAR data, which are used in the classification [32–34], extraction [35,36], monitoring [37,38], and spectral analysis [39,40] of surface features of tidal flats. Optical remote sensing data has the characteristics of multi-temporal, short cycle and wide coverage and has already been used in the sediments extraction of tidal flats [41,42]. And Jung et al. [33] suggested that the multispectral optical sensor is suitable for the classification of the sediments and vegetation in the tidal flats. In addition, in terms of the impact of laver aquaculture, relevant research was only found in He, et al. [43], which adopted field measurement to quantitatively invest impacts of laver cultivation on sedimentary evolution of tidal flats in Rudong, Jiangsu Province but difficult to cover the whole aquaculture regions along the central Jiangsu coast and establish a short-interval time series to analyze evolution patterns. In addition, it is significant to explore the evolution processes caused by laver cultivation due to the unique seasonality, other than biotic processes [44].

The purpose of this study is to investigate the sedimentary evolution of tidal flats in response to laver cultivation using a time series strategy that employs satellite remote sensing images. Taking the central Jiangsu coast as the study area, with the support of remote sensing (RS), a geographic information system (GIS) and numerical simulation technologies, we employed the waterline method to construct digital elevation models (DEMs) of the central Jiangsu coast based on RS images. We analyzed the expansion of aquaculture after producing a series of spatial distribution maps of the laver aquaculture regions and explored the influence of these activities on the sedimentary evolution of tidal flats, in order to enhance the sustainable development of the coast.

2. Materials

2.1. Study Area

The central Jiangsu coast is a typical muddy tidal flat region, ranging from the Xinyang Port to the Xiaoyangkou Port (Figure 1a). The largest tidal sand ridges, the South Yellow Sea Radial Sand Ridges (SYSRSR), are offshore and cover more than 5000 km^2 [45]. The tidal regime is characterized by irregular semi-diurnal tides with a mean tide range varying from 2.5 to 4.0 m [46]. The sediment is composed mainly of silt and sand with the mean grain size ranges from 2.5φ to 7.1φ [47]. Seasons are distinctly defined with spring lasting from March to May, summer from June to August, autumn from September to November and winter from December to February. The central Jiangsu coast is a natural choice for large-scale aquaculture and is an extremely significant seafood farming area in China, especially for laver. Laver cultivation in Jiangsu started in the early 1970s and the aquaculture regions have appeared on satellite images since 1999. Laver cultivation requires a sea area that is below the neap high tide with an unimpeded trend and a slight wind. Hence, laver aquaculture regions are mainly distributed in the lower part of tidal flats and the seaward areas of sand ridges (Figure 1b). Figure 1e–l show that, when the tide fades out of the sand ridges, regularly distributed long strips of surface features can be observed clearly from the RS images and when the tide rises and covers the sand ridges, such features are still visible. The extension direction of these features is almost consistent with the direction of tidal fluctuations. The laver growth period is mostly during winter and spring while the specific time of seeding depends on the water temperature and air temperature. Therefore, laver aquaculture regions can be observed in satellite images obtained during winter and spring only.

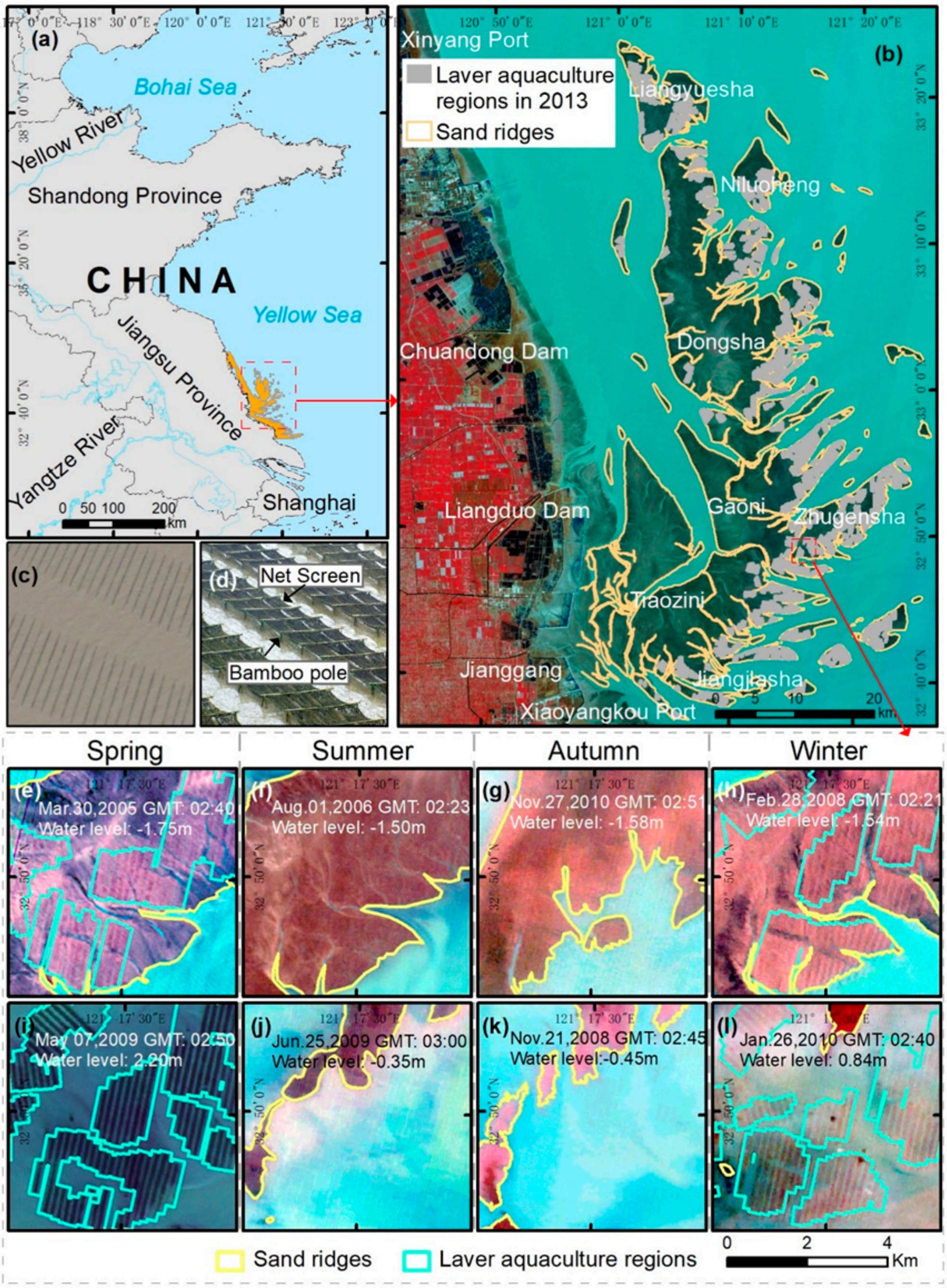

Figure 1. Location and distribution of laver cultivation regions in the central Jiangsu coast. (**a**) The location of the central Jiangsu coast; (**b**) optical image with standard false coloring of the central Jiangsu coast taken by HJ-1B CCD on 1 January 2013 and the laver aquaculture regions in 2013; (**c**), (**d**) the laver aquaculture regions observed from Google Earth and field investigations; (**e**)–(**h**), (i)–(**l**) the aquaculture regions observed from optical images with low and high water levels taken in spring, summer, autumn and winter, respectively. The datum of water levels is the mean sea level.

2.2. Data Set

The data sets used in this study included satellite images, water level records and pre-processed auxiliary data.

2.2.1. Satellite Images

A total of 662 satellite images covering the study area in 1999–2013 were collected from different platforms, including Landsat Thematic Mapper (TM), Landsat Enhanced Thematic Mapper (ETM+), HJ-1A/B Charge Coupled Device (CCD), CBERS CCD, IRS-P6 Advanced Wide-Field Sensor (AWiFS), IRS-P6 Linear Imaging Self-Scanning Sensor (LISS) and BeiJing-1 CCD. The spatial resolution of these satellite images varies from 10 m to 56 m. To assess the locations of laver aquaculture regions, 50 images taken from 1999 to 2013 were used (Table 1), while 160 images taken from December 2008 to August 2010 were employed for DEM construction including six images were used for determination of aquaculture regions as well. All satellite images used are of high quality and show the laver aquaculture regions quite clearly.

It is noted that common medium resolution satellites such as Landsat-5, have a revisit interval of 16 days [48]. The temporal resolution is incapable to meet the requirement of a seasonal scale DEM construction thus, we were unable to carry out a seasonal pattern analysis using these satellites. The HJ-1 satellite constellation, consisting of HJ-1 A and B (launched in 2008) and HJ-1 C (launched in 2012), revisits China and its surrounding areas in intervals of less than 48 h [49], which greatly improved the possibility of seasonal scale DEM construction using optical images. A total of 392 optical images covering the study area recorded by the HJ-1A/B satellites were obtained. Of these, 141 images met the requirements for constructing a DEM, accounting for 35.97% of the total number of collected images. Among the usable images, 98 were considered high quality as the images were cloud-free and the waterlines were distinguishable. In view of 43 images with medium or poor quality, an additional 19 images were added to nearly achieve an average of 23 images per season. The spatial and temporal accuracy of our DEM was guaranteed based on the combination of satellite images from multiple sources.

2.2.2. Water Level Records

Continuous observation records of the water level in Dafeng Port, Lanshayang, Xiaoyangkou Port and Xinyang Port were collected, as well as the forecast water levels from the Jiangsu coastal tidal gauge stations (Sheyang river mouth tidal gauge station, Chenjiawu tidal gauge station, Jianggang tidal gauge station and Lvsi tidal gauge station), to validate the hydrodynamic model simulation results.

2.2.3. Pre-Processed Auxiliary Data

Digital raster maps of the land areas (with a scale of 1:50,000) were used to facilitate geo-correction of the satellite images.

Table 1. Summary of images used for extraction of laver aquaculture regions.

No.	Acquisition Time a) yy-mm-dd hh:mm	Sensor	Tide Level b) (m)	No.	Acquisition Time a) yy-mm-dd hh:mm	Sensor	Tide Level b) (m)
1	19 February 1999 02:10	Landsat5 TM	−1.89	26	14 April 2005 02:51	IRS-P6 LISS3	-1.91
2	12 December 1999 02:06	Landsat7 ETM+	−1.59	27	15 December 2005 02:36	CEBRS CCD	1.09
3	20 December 1999 02:05	Landsat5 TM	2.13	28	29 March 2006 02:33	CEBRS CCD	0.40
4	22 February 2000 02:04	Landsat5 TM	−1.17	29	08 January 2007 02:25	Landsat5 TM	−1.78
5	01 March 2000 02:23	Landsat7 ETM+	0.87	30	09 January 2007 02:25	CEBRS CCD	−1.62
6	09 March 2000 02:04	Landsat5 TM	−1.89	31	02 January 2008 02:56	IRS-P6 AWIFS	0.04
7	15 January 2001 02:21	Landsat7 ETM+	−1.24	32	10 February 2008 02:44	IRS-P6 LISS3	−1.93
8	08 February 2001 02:10	Landsat5 TM	−0.56	33	17 February 2008 02:51	CEBRS CCD	1.28
9	12 March 2001 02:10	Landsat5 TM	−1.92	34	28 February 2008 02:21	Landsat5 TM	−1.38
10	13 April 2001 02:10	Landsat5 TM	−1.64	35	13 January 2009 02:15	Landsat5 TM	−1.96
11	23 November 2001 02:10	Landsat5 TM	−0.32	36	28 January 2009 02:49	HJ1A CCD	−1.35
12	02 January 2002 02:19	Landsat7 ETM+	−1.60	37	06 March 2009 02:53	HJ1B CCD	0.49
13	19 February 2002 02:19	Landsat7 ETM+	−1.16	38	07 May 2009 02:50	HJ1B CCD	2.26
14	08 April 2002 02:19	Landsat7 ETM+	1.43	39	26 January 2010 02:40	HJ1B CCD	0.83
15	05 January 2003 02:19	Landsat7 ETM+	−1.52	40	21 February 2010 02:54	HJ1A CCD	−1.69
16	13 January 2003 02:02	Landsat5 TM	0.89	41	10 March 2010 02:43	HJ1B CCD	0.55
17	21 January 2003 02:19	Landsat7 ETM+	−1.82	42	07 March 2011 02:52	HJ1A CCD	−1.86
18	29 January 2003 02:03	Landsat5 TM	1.82	43	26 March 2012 02:41	HJ1B CCD	−1.98
19	06 February 2003 02:19	Landsat7 ETM+	−1.75	44	28 March 2012 02:42	HJ1A CCD	−0.79
20	18 March 2003 02:04	Landsat5 TM	−1.03	45	31 March 2012 02:23	HJ1A CCD	0.13
21	26 March 2003 02:19	Landsat5 TM	0.16	46	23 April 2012 02:38	HJ1A CCD	0.68
22	13 January 2004 02:41	CEBRS CCD	−2.64	47	30 January 2013 02:17	HJ1A CCD	−1.74
23	08 February 2004 02:41	CEBRS CCD	−0.90	48	03 March 2013 02:04	HJ1B CCD	0.21
24	04 March 2004 02:09	Landsat5 TM	0.86	49	10 April 2013 02:01	HJ1B CCD	1.05
25	30 March 2005 02:40	CEBRS CCD	−1.62	50	11 May 2013 02:11	HJ1B CCD	−0.98

a) The acquisition time is Greenwich Mean Time (GMT). b) Tide level is water level of the Jianggang tidal gauge station (datum: mean sea level).

3. Methods

3.1. Tidal Flat DEM Construction

In this study, the satellite images were taken as inputs. A method of image preprocessing was employed including image filtering, enhancement, geometric correction and segmentation operations. The binary images of tidal flats were extracted and the vector waterlines were constructed from the processed images. It is worth noting that, waterlines in laver aquaculture regions were still extracted along the edge of sandbanks. A marine hydrodynamic simulation model in the coastal area of central Jiangsu Province was adopted and run to simulate the water levels, with inversion of the water levels at 5 min intervals. The observed and forecast water level data from the tidal gauge stations and the satellite altimetry data (Jason-1) were used to validate the hydrodynamic model simulation results. All waterlines were resampled into points at 30 m intervals and linked to the hydrodynamic model to obtain the elevation of each water point. The cell size of DEMs was set to 60 m as the resolution of the satellite images varied from 10 to 56 m. Then, a gridded DEM of the tidal flats in the central Jiangsu coast was created from the discrete points of waterlines using the Kriging interpolation (Figure 2a). More details about the DEM construction can be found in the work of Liu, Li, Cheng, Li and Chen [45].

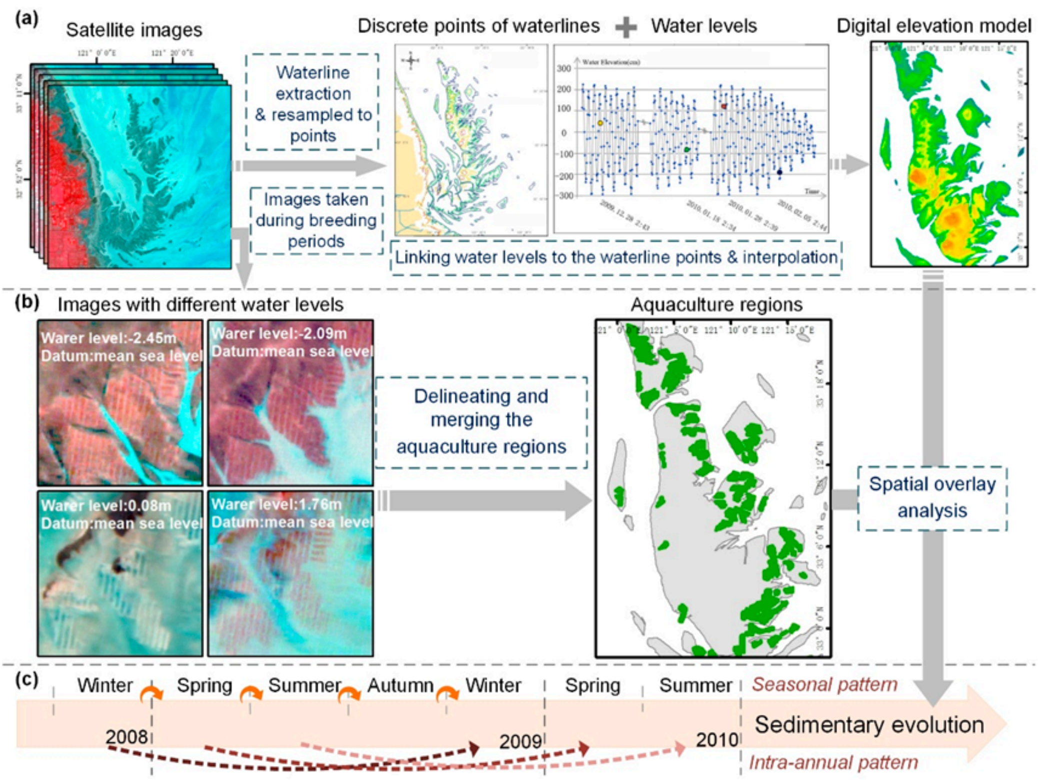

Figure 2. Flow chart illustrating the methodology used in this study. (**a**) Digital elevation model construction; (**b**) aquaculture region extraction; and (**c**) sedimentary evolution based on a time series.

Seven seasonal scale DEMs were established using the waterline method based on multi-temporal RS images. The time periods are December 2008—February 2009, March 2009—May 2009, June 2009—August 2009, September 2009—November 2009, December 2009—February 2010, March 2010—May 2010 and June 2010—August 2010, representing seven seasons as follows winter 2008, spring 2009, summer 2009, autumn 2009, winter 2009, spring 2010 and summer 2010 (Figure 3). The accuracy of DEMs has been validated in a previous study and the mean error is 45.13 cm [50]. The main error sources in building tidal flat DEMs are from water level heighted process and interpolating process [51].

These DEMs provide the foundation for seasonal and intra-annual pattern analysis of the impact of laver cultivation on tidal flat sediment.

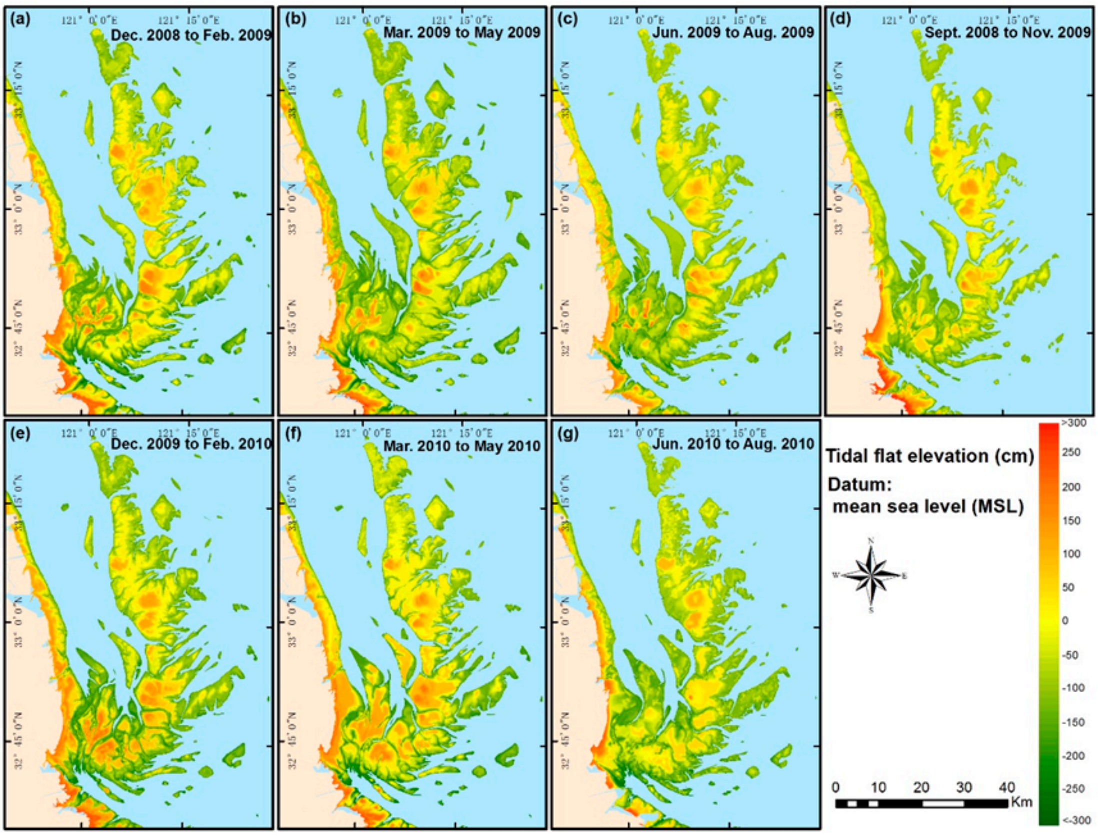

Figure 3. DEMs of the central Jiangsu coast from December 2008 to August 2010. (**a**) Winter 2008 (December 2008 to February 2009); (**b**) spring 2009 (March to May, 2009); (**c**) summer 2009 (June to August, 2009); (**d**) autumn 2009 (September to November, 2009); (**e**) winter 2009 (December 2009 to February 2010); (**f**) spring 2010 (March to May, 2010); and (**g**) summer 2010 (June to August, 2010). The datum of the DEMs is the mean sea level.

3.2. Extraction of Laver Aquaculture Regions

Clear and cloud-free images during the laver growing season, January–May and November–December, were selected. The exposure of aquaculture regions differs at diverse water levels. When tidal levels increase and the sand ridges are submerged, the aquaculture regions are still exposed to the sea surface due to the height of the stent. Therefore, images with a high tidal level and little exposed sand ridges were selected because the aquaculture regions and seawater contract more obviously and are more differentiated after the specific band combination and stretch. When the tidal level recedes, the sand ridges emerge and the aquaculture regions are exposed completely. Thus, images with a low tidal level and completely exposed sand ridges were also employed to supplement the observed inundated regions obtained from images taken at a high tidal level. The polyline data of the aquaculture regions were obtained by vectorizing and merging the selected images (Figure 2b). According to the width of a row of float raft (ranging from 150 m to 180 m) and separation distance of adjacent float rafts (70 m), 150 m buffer zones were established and dissolved to constitute the polygon data of the aquaculture regions from 1999 to 2013. Moreover, the area of the aquaculture was calculated to analyze the trends in spatial expansion.

3.3. Analysis of Tidal Flat Sedimentary Evolution

Tidal flat sediment volume is an important parameter and quantitative index of the sedimentary environment, which comprehensively reflects the characteristics of the erosion and deposition process. The method used to calculate the sediment volume first required dividing the tidal flat into different elevation partitions and then calculating the sediment in each partition. Detailed calculations of these two stages are as follows:

(1) Determination of the elevation partitions. In order to dissect the characteristics of tidal flat sediment in different elevation partitions, it was necessary to determine each elevation partition. The first step was to ascertain the maximum value, N (m), among the minimum elevation values acquired from each constructed DEM and the maximum elevation value M (m) of all the DEMs. Based on these two values (N and M), several elevation partitions can be defined at 0.1 m elevation intervals. These different elevation partitions are N − M, (N + 0.1) − M, (N + 0.2) − M . . . (M − 0.1) − M, respectively.

(2) Quantitative calculation of sediment in each elevation partition. In accordance with the calculation formula, the sediment amount, S = ρ × V, where ρ represents the sedimentary density and V is the sedimentary volume. Since the composition of the tidal flats in the central Jiangsu coast is relatively uniform, the sedimentary density is assumed to be equal in all tidal flat zones. Therefore, the variation of volume is proportional to the variation of sediment amount. Sedimentary volumes are used to characterize tidal flat depositional changes. The spatial resolution of the constructed tidal flat DEMs is 60 m and the area of each grid (3600 m^2) was multiplied by the relative elevation of the grid to determine the volume of the grid. Provided n be the elevation value of the DEM, when $n_i > N$ and the number of grids greater than N is p, the volume V of the elevation partition N − M is:

$$V = \sum_{i=0}^{P} 3600 \cdot (n_i - \mathrm{N}) \tag{1}$$

4. Results

4.1. Expansion of Aquaculture Regions

From the perspective of spatial expansion, laver aquaculture regions were distributed only in the Jiangjiasha sandbank and the southern coast in 1999, which covered only 11.99 km^2 initially calculated from satellite images. With the continuous development of cultivation technology, the aquaculture regions gradually expanded to the north and peripheral regions of the sand ridges. In 2006, the entirety of the aquaculture regions were distributed in the seaward margins of the sand ridges but since 2007, these regions were detected in the landward margins as well. However, landward aquaculture regions tended to be quite disperse and the quantity began decreasing after 2011. Until 2013, the periphery of the Liangyuesha sandbank, the seaward margins of the Dongsha sandbank, the seaward margins of the Gaoni sandbank, the Zhugensha and the Jiangjiasha sandbanks became serried aquaculture regions (Figure 4a–e). While from the view of area extension, the aquaculture regions has been increasing since 1999 and reached 298.28 km^2 by 2013. In 1999–008, the area grew rapidly at an average rate of 28.21 km^2/y. The growth rate reached a crest value of 76.75 km^2 within one year during 2007 to 2008. During 2008–2013, the rate increase diminished to an average of only 6.48 km^2/y (Figure 4f).

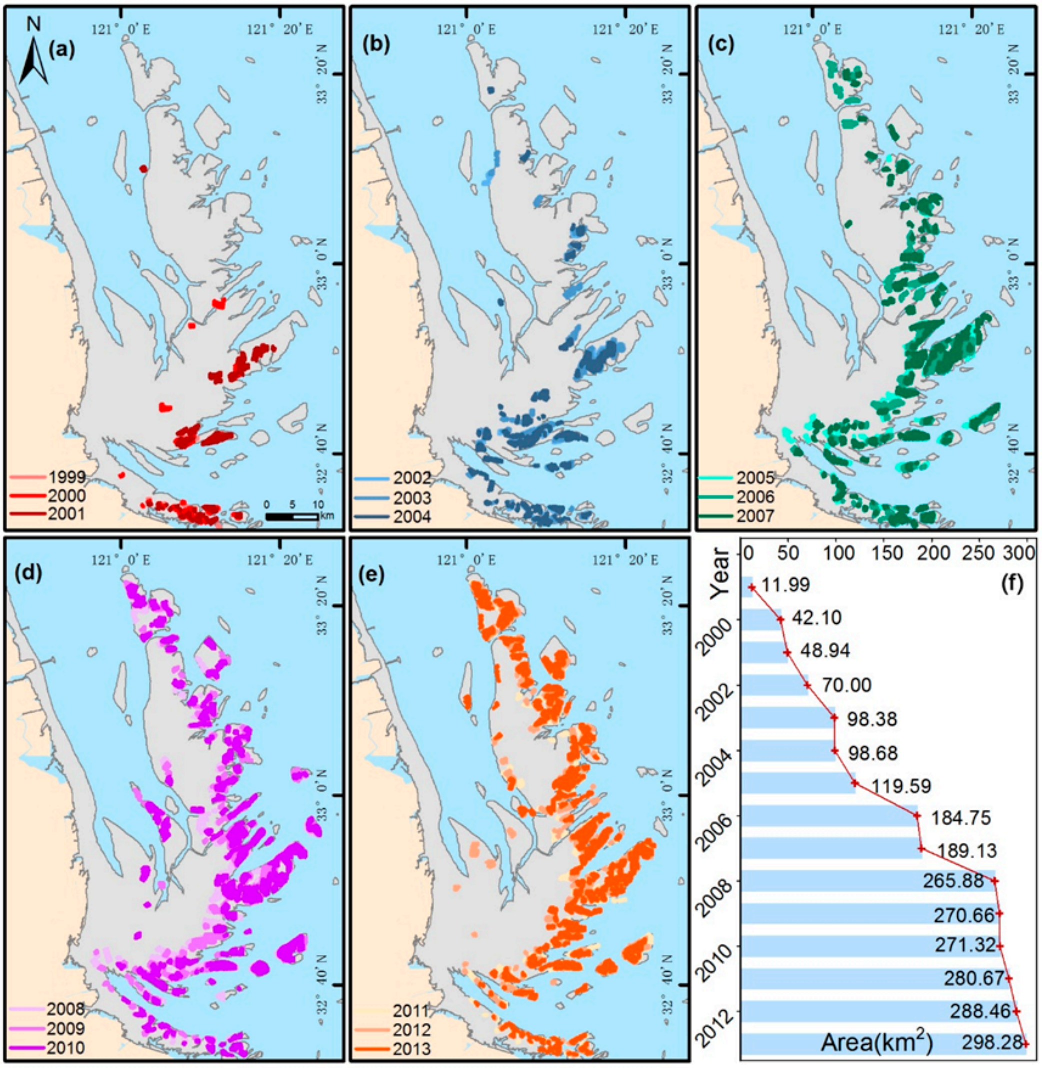

Figure 4. The expansion of the laver aquaculture regions from 1999 to 2013. (**a**)–(**e**) Spatial distribution of the aquaculture regions and (**f**) the growth curve of the area.

4.2. Seasonal Evolution Patterns

In this study, the laver aquaculture regions were separated from the non-aquaculture regions and the sedimentary volume in different elevation intervals was calculated independently. The results show that the seasonal sedimentary evolution patterns of aquaculture regions were more complicated than non-aquaculture regions. From winter 2008 to spring 2009 (the end of the growth period of laver), aquaculture regions of the entire study area were in deposition below −100 cm and in erosion above it. During spring 2009 to summer 2009 (non-growth period), aquaculture regions eroded simply. From summer 2009 to autumn 2009 (the prime growing period), aquaculture regions were in erosion below −90 cm while in deposition above it and were in deposition simply during autumn 2009 to winter 2009 (growth period). In contrast to aquaculture regions, non-aquaculture regions were in erosion from winter 2008 to summer 2009 and in deposition from summer 2009 to winter 2009 (Figure 5a,b). Contrasting the curves of winter 2008 and winter 2009, the aquaculture regions have a demarcation point of −40 cm, where the low tidal flats are in erosion and the high tidal flats are in deposition. However, the variation of the non-aquaculture regions were slight. These results show that the entire study area follows a pattern where low tidal flats were in erosion and high ones in deposition, indicating that the change of scouring and silting caused by laver cultivation was the dominant factor. This result will be expounded specifically in Section 4.3. In addition, the sedimentary evolution patterns of each sandbank is as follows:

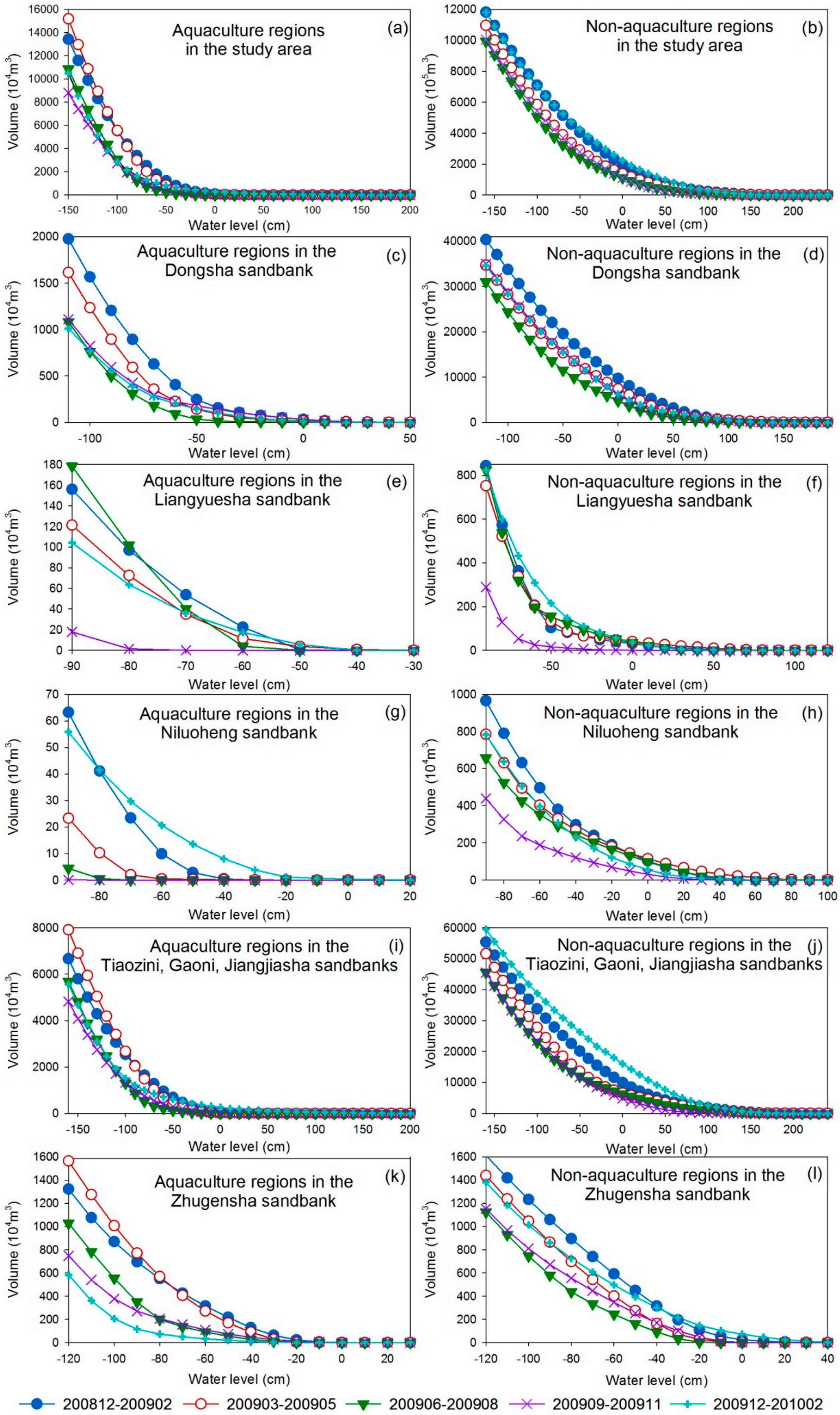

Figure 5. Seasonal patterns of tidal flats in aquaculture and non-aquaculture regions of the central Jiangsu coast. (**a**,**b**) The entire study area; (**c**,**d**) the Dongsha sandbank; (**e**,**f**) the Liangyuesha sandbank; (**g**,**h**) the Niluoheng sandbank; (**i**,**j**) the Tiaozini, Gaoni and Jiangjiasha sandbanks; and (**k**,**l**) the Zhugensha sandbank. The datum of the water levels is the mean sea level.

(1) The Dongsha sandbank (Figure 5c,d). The aquaculture region is principally distributed in the eastern part of this sandbank. The laver growing period is from December to May (from winter to spring), with the aquaculture region undergoing erosion. Both aquaculture and non-aquaculture regions are eroded from spring to summer, while undergoing deposition from summer to autumn. From autumn to winter, the aquaculture region reveals little erosion and the non-aquaculture region exhibits slight deposition. Thus, the sediment volume of both regions during autumn to winter was nearly unchanged.

(2) The Liangyuesha sandbank (Figure 5e,f). This sandbank is located in the northern part of the study area with peripherally distributed aquaculture regions. Therefore, the sediment volume variations of the aquaculture and non-aquaculture regions are similar. The laver growth period is from November to June (from autumn to spring). From autumn to winter, the aquaculture and non-aquaculture regions are in deposition while from winter to spring, the two areas experience deposition above −50 cm and erosion below −50 cm. During the non-culture period (from spring to autumn), the aquaculture region is in erosion above −70 cm and in deposition below −70 cm to keep its scouring and silting balance from spring to summer. Simultaneously, the non-aquaculture region experiences moderate siltation within −50cm~ 0 cm with sedimentary evolution almost invariable in the remaining elevation ranges. The both two regions erode from summer to autumn and the sediment volume reaches a minimum in the autumn.

(3) The Niluoheng sandbank (Figure 5g,h). The sandbank is located in the periphery of the radial sand ridges with minimal area and poor stability. The laver growing period is from December to May (from winter to spring). The aquaculture region is mainly distributed in the southern sandbank and appears alluvial from autumn to winter and erosive in the other periods. The non-aquaculture region is in deposition between winter and spring and the sediment variation is identical with that of the aquaculture region in the other time. Similar to the Liangyuesha sandbank, the volume of both two regions reduces to the minimum in the autumn.

(4) The Tiaozini, Gaoni and Jiangjiasha sandbanks (Figure 5i,j). These three inner sandbanks are connected to the land with excellent stability. The aquaculture region is located on the seaside margins. Laver is cultivated from October to May (from autumn to spring) and the aquaculture region in this period is alluvial below −90 cm (from winter to spring) and above −100 cm (from autumn to winter), compared to the non-aquaculture region which is simply in erosion. Meanwhile, from June to September (from spring to summer), the sediment variation of the two regions both appears erosion.

(5) The Zhugensha sandbank (Figure 5k,l). The aquaculture region is distributed on the beach surface of the peripheral sandbank. Laver cultivation occurs from December to June (from winter to spring). During the growing period, the aquaculture region deposits below −80 cm compared to the non-aquaculture region which erodes. Within the non-culture period, these two regions are in erosion between spring and summer. The aquaculture region deposits above −80 cm while erosion occurs below −80 cm from summer to autumn, contrary to the growing period and is in erosion from autumn to winter. Moreover, the non-aquaculture region undergoes silting from summer to winter.

4.3. Intra-Annual Evolution Patterns

Comparing the curves of winter 2008 and winter 2009, the study area and all the sandbanks except the Dongsha and Zhugensha sandbanks appear to undergo siltation in the high tidal flats and erosion in the low tidal flats. Due to the geographical location, hydrodynamic conditions and sedimentary environment, the erosion and deposition evolution of each sandbank differs. Hence, the entire study area was taken as a single object, contrasting the sedimentation volume of the aquaculture regions and non-aquaculture regions during three periods (winter 2008 vs. winter 2009, spring 2009 vs. spring 2010, summer 2009 vs. summer 2010). The curves in Figure 6 indicate that in the aquaculture regions, the high tidal flats undergo siltation and the low tidal flats undergo erosion, while the non-aquaculture regions do not follow this pattern. From winter 2008 to winter 2009, the demarcation point of the aquaculture region is at −40 cm. The non-aquaculture region erodes and deposits slightly, with the two processes in approximate balance (Figure 6a,b). From spring 2009 to spring 2010, the aquaculture region is delimited by −130 cm, nevertheless, the non-aquaculture region appears to undergo siltation. Between summer 2009 and summer 2010, the aquaculture region is divided by −80 cm, while the non-aquaculture region erodes. Laver cultivation makes the high tidal flats more susceptible to siltation and thus, the convex beach surface is gradually shaped.

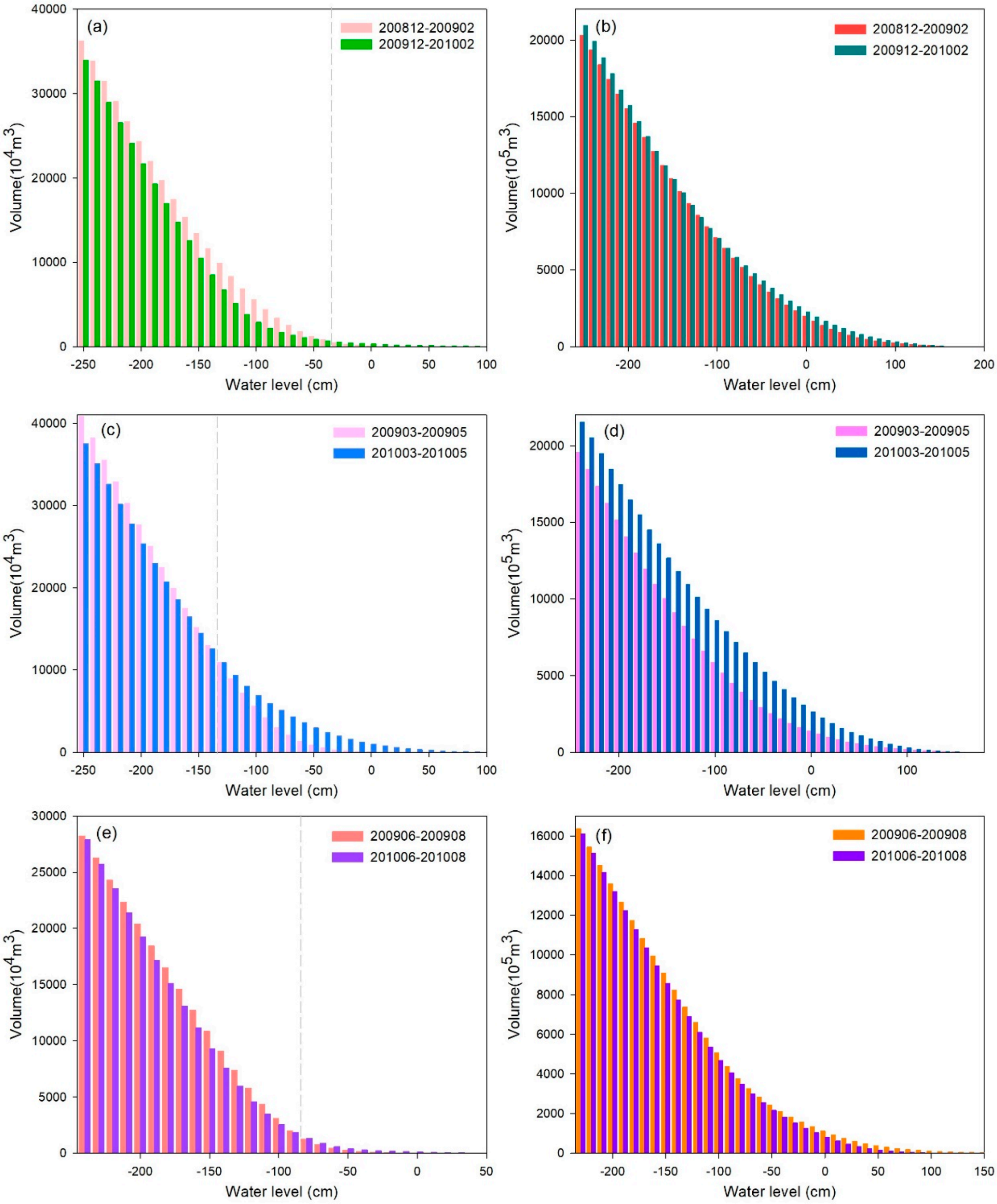

Figure 6. Intra-annual patterns of tidal flats in aquaculture and non-aquaculture regions of the study area. During winter 2008 vs. winter 2009, respectively in (**a**) aquaculture and (**b**) non-aquaculture regions; During spring 2009 vs. spring 2010, respectively in (**c**) aquaculture and (**d**) non-aquaculture regions; During summer 2009 vs. summer 2010, respectively in (**e**) aquaculture and (**f**) non-aquaculture regions. The datum of the water levels is the mean sea level.

5. Discussion

This research realizes the analysis of the quarterly and annual influence patterns of laver aquaculture on the sedimentary evolution of tidal flats in the central Jiangsu coast, based on the long time series remote sensing images, by extracting the laver aquaculture regions, simulating the construction of tidal flat DEMs and using different elevation intervals to calculate the sedimentary volumes. With the increase of the number of optical remote sensing images, the time resolution of image analysis is improved, which accelerates our analysis of the sedimentary evolution of tidal flats with seasonal scale, which is different from the most existing tidal flat researches in the annual time unit [52]. Moreover, most of the current researches are aimed at the evolution or classification of biomass or non-biomass substances produced under the natural environment of tidal flats [52–54] and our research focuses on the effects of human activities (laver aquaculture) on the sedimentary evolution of tidal flats, which is helpful for subsequent studies of more detailed analysis of tidal flats. However, considering the uncertainty of the research method, including the availability of remote sensing images and the diversified factors affecting the evolution patterns of tidal flats.

5.1. The Availability of Remote Sensing Images

Laver cultivation reveals a seasonal cycle, with a growing period spanning from winter to spring and a non-growing period from summer to autumn. Thus, the influence of laver cultivation on the tidal flat sediment is more obvious on the seasonal scale, especially before and after the establishment and demolition of the structures required for aquaculture. Impacted by the Jiang-huai quasi-stationary front (in June and July), images recorded in summer (from June to September) are heavily cloud-covered and the number of available images is significantly less than that of winter (from December to February). Thus, for coastal zones with complex depositional dynamics and rapidly varying topography, the availability of optical images is restricted when analyzing the characteristics of tidal flats geomorphic evolution within a short time. With the development of RS technology and improvements in the spatial and temporal resolution of satellite images, it will be possible to construct monthly-scale or even day-scale DEMs corresponding to the periods of laver sowing, growth and frame set up and demolition. With this data, more regular conclusions may be inferred.

Meanwhile, the Synthetic Aperture Radar (SAR) data with all-weather day-night [55] capability compensates for the absence of optical images caused by imaging quality, such as ENVISAT, ESR, Sentinel satellites launched by European Space Agency (ESA). Therefore, coalescing multisource RS data such as optical images with ultra-high temporal resolution and SAR data will provide data support for inverting the changing terrain of tidal flats terrain.

5.2. The Diversified Factors Affecting the Evolution Patterns of Tidal Flats

The sedimentary evolution of the aquaculture and non-aquaculture regions of each sandbank is heterogeneous due to their different locations, hydrodynamic conditions and distribution of laver cultivation. Hydrodynamics plays a significant role in affecting sediment transport and appears seasonal variations [46]. Impacted by the monsoon climate, rough sea conditions in the sea north of Jianggang port caused by cold waves in autumn and winter play a leading role in the partial sediment transition [56], while typhoon waves in summer affect southern part of radial sandbanks mainly. Taken the Jianggang port as the boundary point, current velocity of north tidal is faster than the south. Moreover, the different distributions of aquaculture regions in each sandbank also influence evolution patterns. The Dongsha and Niluoheng sandbanks show an atypical erosion-and-deposition cycle, because in both sandbanks the aquaculture regions are distributed in the seaside margins. The billow caused by cold waves brings sediment out from the aquaculture regions during the growing period (from winter to spring), leading to sedimentary erosion but not siltation in the aquaculture regions. The aquaculture region of the Liangyuesha sandbank is relatively evenly distributed in the periphery and the sediment supply from peripheral sandbanks is one of the sources of inner sandbank sediment [57].

Thus the deposition and erosion keeps balance generally and a typical sedimentary evolution pattern was observed. The Tiaozini, Gaoni and Jiangjiasha sandbanks and the Zhugensha sandbank have excellent stability and are located in the sedimentary convergent center leading to a typical sediment evolution arising from laver cultivation.

It is worth noting that the rhythmic results of this study are only derived from satellite images. Evolution patterns of Jiangsu coast will be analyzed based on space/aerial/ground remote sensing technologies in further study. Combined with Synthetic Aperture Radar (SAR), terrestrial laser scanning and drones, we will acquire field observation data and optimize the accuracy of DEM to derive more regular results.

6. Conclusions

The stability of the tidal flats is of great significance to ecological protection and marine development. In the context of the increasingly frequent human activities, understanding its impact on morphology of tidal flats provides scientific evidence for sustainable development. In the central Jiangsu coast, laver aquaculture regions have been expanding and have exerted a remarkable impact on the tidal flats. In this study, combined with seven seasonal DEMs of the tidal flats in the central Jiangsu coast, the seasonal and intra-annual sedimentary evolution patterns were analyzed. The three major conclusions are summarized below.

(1) Laver aquaculture regions were distributed only in the Jiangjiasha sandbank and the southern coast in 1999 and have gradually expanded to the north and peripheral regions of the all sand ridges. Until 2013, the aquaculture regions were located on the seaward margins. The aquaculture regions increased from 11.99 km^2 to 295.28 km^2.

(2) Seasonal sedimentary evolution patterns with deposition during winter and erosion during summer were observed. The aquaculture regions experience deposition in certain elevation intervals compared to monotonic erosion changes observed in non-aquaculture regions during the growing period. In the non-growing period, the aquaculture regions erode at alluvial elevation intervals and deposit at erosive ones in order to maintain the balance of scouring and silting.

(3) Intra-annual sedimentary evolution comprised sedimentary deposition in the high tidal flats and erosion in the low ones. The monolithic morphology and macroscopic evolution of sandbanks are principally the result of natural factors such as hydrodynamic conditions and human activities such as laver cultivation, which makes deposition on the high tidal flats more favorable eventually leading to gradual changes in beach surface topology.

Author Contributions: Y.L. (Yongxue Liu), J.S. and W.L. conceived and designed the experiments; W.L. and J.S. performed the experiments; W.L. and J.S. analyzed the data; Y.L. (Yongchao Liu) and B.Z. contributed materials; W.L. and J.S. wrote the paper; Y.L. (Yongxue Liu), W.L. and Yongchao Liu edited the text.

Funding: This research was supported by the Jiangsu Provincial Natural Science Foundation (No. BK20160023), the National Natural Science Foundation of China (No. 41471068), and the Open Fund of Key Laboratory of Coastal Zone Exploitation and Protection, Ministry of Natural Resources of China (No:2017CZEPK12).

Acknowledgments: We thank the three anonymous reviewers and the associate editor for their constructive suggestions for improving the manuscript.

Conflicts of Interest: The author declares no conflict of interest.

References

1. Chen, J.Y.; Cheng, H.Q.; Dai, Z.J.; Eisma, D.K. Harmonious development of utilization and protection of tidal flats and wetlands-a case study in Shanghai Area. *China Ocean Eng.* **2008**, *22*, 649–662.
2. Zone, L.O.I.I.; Kremer, H.H.; Tissier, M.D.A.L.; Burbridge, P.R.; Talaue-Mcmanus, L.; Rabalais, N.N.; Parslow, J.; Crossland, C.J.; Young, B. Land-ocean interactions in the coastal zone: Science plan and implementation strategy. *Environ. Policy Collect.* **2005**, *20*, 1262–1268.

3. Zhu, Q.; Yang, S.; Ma, Y. Intra-tidal sedimentary processes associated with combined wave–current action on an exposed, erosional mudflat, southeastern Yangtze river delta, China. *Mar. Geol.* **2014**, *347*, 95–106. [CrossRef]
4. Ramesh, R.; Chen, Z.; Cummins, V.; Day, J.; D'Elia, C.; Dennison, B.; Forbes, D.L.; Glaeser, B.; Glaser, M.; Glavovic, B.; et al. Land-ocean interactions in the coastal zone: Past, present and future. *Anthropocene* **2015**, *12*, 85–98. [CrossRef]
5. Liu, Y.X.; Li, M.C.; Mao, L.; Cheng, L.; Li, F.X. Toward a method of constructing tidal flat digital elevation models with modis and medium-resolution satellite images. *J. Coast. Res.* **2013**, *29*, 438–448. [CrossRef]
6. Pendleton, L.; Donato, D.C.; Murray, B.C.; Crooks, S.; Jenkins, W.A.; Sifleet, S.; Craft, C.; Fourqurean, J.W.; Kauffman, J.B.; Marbà, N. Estimating global "blue carbon" emissions from conversion and degradation of vegetated coastal ecosystems. *PLoS ONE* **2012**, *7*, e43542. [CrossRef] [PubMed]
7. Kirby, J.R.; Kirby, R. Medium timescale stability of tidal mudflats in bridgwater bay, bristol channel, uk: Influence of tides, waves and climate. *Cont. Shelf Res.* **2008**, *28*, 2615–2629. [CrossRef]
8. Xu, J.X. Response of land accretion of the yellow river delta to global climate change and human activity. *Quat. Int.* **2008**, *186*, 4–11. [CrossRef]
9. Syvitski, J.P.; Kettner, A.J.; Overeem, I.; Hutton, E.W.; Hannon, M.T.; Brakenridge, G.R.; Day, J.; Vörösmarty, C.; Saito, Y.; Giosan, L. Sinking deltas due to human activities. *Nat. Geosci.* **2009**, *2*, 681–686. [CrossRef]
10. Blum, M.D.; Roberts, H.H. Drowning of the mississippi delta due to insufficient sediment supply and global sea-level rise. *Nat. Geosci.* **2009**, *2*, 488–491. [CrossRef]
11. Rao, K.N.; Subraelu, P.; Kumar, K.C.V.; Demudu, G.; Malini, B.H.; Rajawat, A. Impacts of sediment retention by dams on delta shoreline recession: Evidences from the krishna and godavari deltas, india. *Earth Surf. Process. Landf.* **2010**, *35*, 817–827. [CrossRef]
12. Yang, S.L.; Milliman, J.D.; Li, P.; Xu, K. 50,000 dams later: Erosion of the Yangtze river and its delta. *Glob. Planet. Chang.* **2011**, *75*, 14–20. [CrossRef]
13. Ren, M.E.; Zhang, R.S.; Yang, J.H.; Zhang, D.C. The influence of storm tide on mud plain coast—With special reference to Jiangsu province. *Mar. Geology Quat. Geology.* **1983**, *3*, 1–24. [CrossRef]
14. Shi, Z.; Chen, J.Y. Morphodynamics and sediment dynamics on intertidal mudflats in China (1961–1994). *Cont. Shelf Res.* **1996**, *16*, 1909–1926. [CrossRef]
15. Fagherazzi, S.; Wiberg, P.L. Importance of wind conditions, fetch, and water levels on wave-generated shear stresses in shallow intertidal basins. *J. Geophys. Res. Earth Surf.* **2009**, *114*. [CrossRef]
16. Flemming, B.W.; Nyandwi, N. Land reclamation as a cause of fine-grained sediment depletion in backbarrier tidal flats (Southern North Sea). *Aquat. Ecol.* **1994**, *28*, 299–307. [CrossRef]
17. Hodoki, Y.; Murakami, T. Effects of tidal flat reclamation on sediment quality and hypoxia in isahaya bay. *Aquat. Conserv. Mar. Freshw. Ecosyst.* **2006**, *16*, 555–567. [CrossRef]
18. Wang, Y.P.; Gao, S.; Jia, J.J.; Thompson, C.E.; Gao, J.H.; Yang, Y. Sediment transport over an accretional intertidal flat with influences of reclamation, Jiangsu coast, China. *Mar. Geol.* **2012**, *291*, 147–161. [CrossRef]
19. Jia, L.W.; Pan, S.Q.; Wu, C.Y. Effects of the anthropogenic activities on the morphological evolution of the modaomen estuary, pearl river delta, China. *China Ocean Eng.* **2013**, *27*, 795–808. [CrossRef]
20. Song, D.H.; Wang, X.H.; Zhu, X.M.; Bao, X.W. Modeling studies of the far-field effects of tidal flat reclamation on tidal dynamics in the East China Seas. *Estuar. Coast. Shelf Sci.* **2013**, *133*, 147–160. [CrossRef]
21. Gao, G.D.; Wang, X.H.; Bao, X.W. Land reclamation and its impact on tidal dynamics in Jiaozhou Bay, Qingdao, China. *Estuar. Coast. Shelf Sci.* **2014**, *151*, 285–294. [CrossRef]
22. Sun, C.; Liu, Y.X.; Zhao, S.S.; Li, H.Y.; Sun, J.Q. Saltmarshes response to human activities on a prograding coast revealed by a dual-scale time-series strategy. *Estuar. Coasts* **2016**, *40*, 522–539. [CrossRef]
23. Yang, S.L.; Chen, J.Y. The role of vegetation in mud coast processes. *Oceanol. Limnol. Sin.* **1994**, *25*, 631–635.
24. Netto, S.A.; Lana, P.C. Influence ofspartina alternifloraon superficial sediment characteristics of tidal flats in paranaguá bay (South-Eastern Brazil). *Estuar. Coast. Shelf Sci.* **1997**, *44*, 641–648. [CrossRef]
25. Wang, A.J.; Gao, S.; Jia, J.J. Impact of the cord-grass spartina alterniflora on sedimentary and morphological evolution of tidal salt marshes on the Jiangsu coast, China. *Acta Oceanol. Sin.* **2006**, *25*, 32–42.
26. Ge, B.M.; Bao, Y.X.; Cheng, H.Y.; Zhang, D.Z. Influence of spartina alterniflora invasion stages on macrobenthic communities on a tidal flat in Wenzhou bay, China. *Braz. J. Oceanogr.* **2012**, *60*, 441–448. [CrossRef]

27. Kang, J.W. Changes in tidal characteristics as a result of the construction of sea-dike/sea-walls in the mokpo coastal zone in Korea. *Estuar. Coast. Shelf Sci.* **1999**, *48*, 429–438. [CrossRef]
28. Byun, D.; Wang, X.; Holloway, P. Tidal characteristic adjustment due to dyke and seawall construction in the mokpo coastal zone, Korea. *Estuar. Coast. Shelf Sci.* **2004**, *59*, 185–196. [CrossRef]
29. Traini, C.; Proust, J.-N.; Menier, D.; Mathew, M. Distinguishing natural evolution and human impact on estuarine morpho-sedimentary development: A case study from the vilaine estuary, France. *Estuar. Coast. Shelf Sci.* **2015**, *163*, 143–155. [CrossRef]
30. Wu, X.; Wang, A. Impacts of human beings' activities on north Jiangsu tidal flat. *Sci. Geogr. Sin.* **2005**, *25*, 614.
31. Song, W.L.; Qian, Y.; Su, X.X. Analysis of ecological impact on Yancheng nature reserves for building Dafeng wind farms. *Adm. Tech. Environ. Monit.* **2011**, *23*, 32–36.
32. Wang, W.; Yang, X.; Liu, G.; Zhou, H.; Ma, W.; Yu, Y.; Li, Z. Random forest classification of sediments on exposed intertidal flats using alos-2 quad-polarimetric sar data. In *XXIII ISPRS Congress, Commission VIII*; Halounova, L., Safar, V., Raju, P.L.N., Planka, L., Zdimal, V., Kumar, T.S., Faruque, F.S., Kerr, Y., Ramasamy, S.M., Comiso, J., et al., Eds.; The International Archives of the Photogrammetry, Remote Sensing and Spatial Information Sciences: Prague, Czech Republic, 2016; Volume XLI-B8, pp. 1191–1194. [CrossRef]
33. Jung, R.; Adolph, W.; Ehlers, M.; Farke, H. A multi-sensor approach for detecting the different land covers of tidal flats in the german wadden sea—A case study at norderney. *Remote Sens. Environ.* **2015**, *170*, 188–202. [CrossRef]
34. Wang, W.; Gade, M. A new sar classification scheme for sediments on intertidal flats based on multi-frequency polarimetric sar imagery. *Int. Arch. Photogramm. Remote Sens. Spat. Inf. Sci.* **2017**, *42*, 223–228. [CrossRef]
35. Adolph, W.; Farke, H.; Lehner, S.; Ehlers, M. Remote sensing intertidal flats with terrasar-x. A sar perspective of the structural elements of a tidal basin for monitoring the wadden sea. *Remote Sens.* **2018**, *10*, 1085. [CrossRef]
36. Geng, X.; Li, X.-M.; Velotto, D.; Chen, K.-S. Study of the polarimetric characteristics of mud flats in an intertidal zone using c- and x-band spaceborne sar data. *Remote Sens. Environ.* **2016**, *176*, 56–68. [CrossRef]
37. Mason, D.C.; Davenport, I.J. Accurate and efficient determination of the shoreline in ers-1 sar images. *IEEE Trans. Geosci. Remote Sens.* **1996**, *34*, 1243–1253. [CrossRef]
38. Al Fugura, A.K.; Billa, L.; Pradhan, B. Semi-automated procedures for shoreline extraction using single radarsat-1 sar image. *Estuar. Coast. Shelf Sci.* **2011**, *95*, 395–400. [CrossRef]
39. Manzo, C.; Valentini, E.; Taramelli, A.; Filipponi, F.; Disperati, L. Spectral characterization of coastal sediments using field spectral libraries, airborne hyperspectral images and topographic lidar data (fhyl). *Int. J. Appl. Earth Observ. Geoinf.* **2015**, *36*, 54–68. [CrossRef]
40. Adolph, W.; Jung, R.; Schmidt, A.; Ehlers, M.; Heipke, C.; Bartholomae, A.; Farke, H. Integration of terrasar-x, rapideye and airborne lidar for remote sensing of intertidal bedforms on the upper flats of norderney (German Wadden Sea). *Geo-Mar. Lett.* **2017**, *37*, 193–205. [CrossRef]
41. Brockmann, C.; Stelzer, K. Optical remote sensing of intertidal flats. In *Remote Sensing of the European Seas*; Springer: Berlin, Germany, 2008; pp. 117–128.
42. Valentini, E.; Taramelli, A.; Filipponi, F.; Giulio, S. An effective procedure for eunis and natura 2000 habitat type mapping in estuarine ecosystems integrating ecological knowledge and remote sensing analysis. *Ocean Coast. Manag.* **2015**, *108*, 52–64. [CrossRef]
43. He, H.C.; Shi, Y.; Yin, Y.; Liu, X.Y.; Li, H.Q. Impact of prophyra cultivation on sedimentary and morphological evolution of tidal flat in Rudong, Jiangsu province. *Quat. Sci.* **2012**, *32*, 1161–1172.
44. Widdows, J.; Brinsley, M. Impact of biotic and abiotic processes on sediment dynamics and the consequences to the structure and functioning of the intertidal zone. *J. Sea Res.* **2002**, *48*, 143–156. [CrossRef]
45. Liu, Y.X.; Li, M.C.; Cheng, L.; Li, F.X.; Chen, K.F. Topographic mapping of offshore sandbank tidal flats using the waterline detection method: A case study on the Dongsha sandbank of Jiangsu radial tidal sand ridges, China. *Mar. Geod.* **2012**, *35*, 362–378. [CrossRef]
46. Xing, F.; Wang, Y.P.; Wang, H.V. Tidal hydrodynamics and fine-grained sediment transport on the radial sand ridge system in the Southern Yellow Sea. *Mar. Geol.* **2012**, *291*, 192–210. [CrossRef]
47. Wang, R.; Zhang, Y.Z.; Xia, F.; Zhao, S.D. Grain size distribution and transportation trends of bottom sediments in the sand ridge field of the South Yellow Sea, China. *Mar. Geol. Quat. Geol.* **2012**, *32*, 2012. [CrossRef]

48. Song, J.W.; Zhang, Y.J.; LI, X.C.; Yang, W.Z. Comparison between gf-1 and landsat-8 images in land cover classification. *Prog. Geogr.* **2016**, *35*, 255–263.
49. Wang, Q.; Wu, C.Q.; Li, Q.; Li, J.S. Chinese hj-1a/b satellites and data characteristics. *Sci. China Earth Sci.* **2010**, *53*, 51–57. [CrossRef]
50. Liu, Y.X.; Li, M.C.; Mao, L.; Cheng, L.; Chen, K.F. Seasonal pattern of tidal-flat topography along the Jiangsu Middle Coast, China, using hj-1 optical images. *Wetlands* **2013**, *33*, 871–886. [CrossRef]
51. Liu, Y.X.; Li, M.C.; Zhou, M.X.; Yang, K.; Mao, L. Quantitative analysis of the waterline method for topographical mapping of tidal flats: A case study in the Dongsha Sandbank, China. *Remote Sens.* **2013**, *5*, 6138–6158. [CrossRef]
52. Taramelli, A.V.E.; Cornacchia, L.; Mandrone, S. Modelling uncertainty in estuarine system by means of combined approach of optical and radar remote sensing. *Coast. Eng.* **2014**, *87*, 77–96. [CrossRef]
53. Taramelli, A.; Valentini, E.; Cornacchia, L.; Monbaliu, J.; Sabbe, K. Indications of dynamic effects on scaling relationships between channel sinuosity and vegetation patch size across a salt marsh platform. *J. Geophys. Res.-Earth Surf.* **2018**, *123*, 2714–2731. [CrossRef]
54. Choi, J.K.; Eom, J.; Ryu, J.H. Spatial relationships between surface sedimentary facies distribution and topography using remotely sensed data: Example from the ganghwa tidal flat, Korea. *Mar. Geol.* **2011**, *280*, 205–211. [CrossRef]
55. Mason, D.C.; Davenport, I.J.; Robinson, G.J.H.; Flather, R.A.; McCartney, B.S. Construction of an inter-tidal digital elevation model by the water-line method. *Geophys. Res. Lett.* **1995**, *22*, 3187–3190. [CrossRef]
56. Wu, Y.C.; Huang, H.J.; Yang, Y.L. Hydraulic dynamical effect on the formation and evolution processes of the deltaic sand banks off northern Jiangsu Coast. *Stud. Mar. Sin.* **1998**, *40*, 55–63.
57. Gao, S.; Wang, Y.P.; Gao, J.H. Sediment retention at the Changjiang sub-aqueous delta over a 57 years period, in response to catchment changes. *Estuar. Coast. Shelf Sci.* **2011**, *95*, 29–38. [CrossRef]